# INSTITUTO DE FÍSICA

# preprint

IFUSP/P-148

## ENERGY DEPENDENCE OF THE EIKONAL IN p-p ELASTIC COLLISION



by

H.M. França and Y. Hama

UNIVERSIDADE DE SÃO PAULO
INSTITUTO DE FÍSICA
Caixa Postal - 20.516
Cidade Universitária
São Paulo - BRASIL

# ENERGY DEPENDENCE OF THE EIKONAL IN p-p ELASTIC COLLISION

H.M.França and Y. Hama

Instituto de Física, Universidade de São Paulo, SP, Brasil

## A B S T R A C T

A careful analysis of the elastic p-p scattering in the energy range $20 \lesssim \sqrt{s} \lesssim 60$ GeV is presented. Under the hypothesis of a pure imaginary amplitude with two zeros, the experimental data suggest that the opacity be parametrized as $\chi(s,b) = \chi_f(b) + \log\frac{s}{s_o}\chi_o(b)$, where the energy dependent term is much wider than $\chi_f(b)$, opposing to the factorization hypothesis and some earlier results. This conclusion is precisely the one predicted by the two-component model which has been proposed in our previous work.

OUT/78

# I. INTRODUCTION

In analysing high-energy hadron-hadron elastic scatterings, it is customary to employ an eikonal model, where the eikonal (or opacity) $\chi$ is somehow related to the matter distribution inside the incident particles. When Chou and Yang[1], first proposed this kind of model, it was everybody's belief that the cross sections were tending to some constant asymptotic values, so that their proposal $\chi \sim \langle F_A F_B \rangle$ (here, $\langle\ \rangle$ indicates two-dimensional Fourier transform and $F_A$ and $F_B$ are the electromagnetic form factors of the two interacting hadrons) was perfectly natural and this relation was expected to be valid as $s \to \infty$.

As the ISR and, more recently, NAL accelerator have begun to work, that belief has dissipated at once and today we know that, as the incident energy rises, the total, inelastic and elastic cross sections slowly but steadily increase. Also, the angular distribution at small t continues to shrink. These energy dependences of cross sections brought a trouble to the earlier Chou-Yang's proposal, since now we do not know just at which energy the above identification (namely $\chi \sim \langle F_A F_B \rangle$) should be done. It seems possible to overcome this difficulty by making as assumption that the opacity factorizes[2], that is,

$$\chi(s,b) \sim f(s)\, \chi_0(b) \qquad (1)$$

and saying that the space-dependent part of $\chi$ is related to the hadronic matter distribution of the incident parti-

cles. We do not know, however, any fundamental reason for this factorization, so it should be carefully examined by comparing with the existent experimental data.

The main object of the present paper is to report the results of a systematic and careful analysis of the published pp elastic data, to compare them with some earlier works and finally to interpret them in terms of our previous work[3].

The plan of presentation is the following. In the next section, we collect all the experimental data which have been used in this analysis, which is described in section III, together with the results. Comparisons with some earlier results and also with some models are carried out in section IV. In section V, we briefly delineate the previously proposed two-component model and, then, compare with the results obtained here.

## II. EXPERIMENTAL DATA

In handling experimental data, we must always have in mind the following two points. First, that they are incomplete, so that some kind of interpolation or extrapolation shall necessarily be done. Moreover, data obtained by different authors are frequently conflicting, showing discrepancies which are often larger than the quoted experimental errors. Thus, we think that, if we limit ourselves to analysing just one group of data, it may end in completely unsufficient results. Also, if we choose two or more groups of data, but do not exercise enough care in observing the overall behavior of each group of data with respect to the others, it may lead to quite erroneous conclusions.

In the present analysis, we have considered essentially all the existing pp elastic data, obtained both at the ISR[4-11] and at the Fermilab[12-15], covering the energy range of $\sqrt{s}$ = 20 ~ 60 GeV. These data may be grouped as follows.

a) Total cross sections: we have used only the more recent accurate NAL data from Ref. 12 and the ISR data obtained by CERN-Pisa-Rome-Stony Brook Collaboration[4]. Actually, there are some older data with large experimental uncertainties and which essentially agree with the data mentioned above. Moreover, the authors of Ref. 4 claim that the new data are results of an improvement of their previous works performed by using the same methods employed now. Thus, we believe the data used by us are representative enough of all the pp cross

section measurements which have ever been done. The two groups of data above are shown in Fig. 1, where one can see that they are approximately on a same curve (or perhaps there is a systematic deviation of ~ 0.5 mb between two groups of data). In using these data for determining the optical point, an interpolation has been made in the transition region.

b) Slope parameters for very small t: There are five independent measurements[5-8,13] which are shown in Fig. 1. In treating these data, one must keep in mind which is the t-interval where each point has been obtained. For instance, at $\sqrt{s}$ = 30 GeV, Ref. 6 gives the slope in the interval $0.015 < -t < 0.055$ GeV$^2$, whereas the data given by Ref. 5 refers to $0.046 < -t < 0.09$ GeV$^2$. This may be the main origin of their discrepancy as they appear in Fig.1, since $B = 13.0 \pm 0.7$ GeV$^{-2}$ is compatible with the data points of Ref. 5 when the t interval is correctly chosen.

c) Normalized angular distributions: there are four independent data[9,10,14,15] in different energy or t intervals, such that no direct consistency check is possible among them. We can see, however, that the data of Refs. 9 and 14 extrapolate correctly down to the small t data mentioned in a) and b).

d) Unnormalized angular distributions: There are two angular-distribution measurements at ISR energies which have not been normalized, but contain valuable informations which are essential in determining the energy-dependent behavior of the amplitude. One is Ref. 5 which gives the angular distributions at small-t for several

energies. As will be discussed later in section IV, the omission of these data may lead to a completely distorted result concerning the energy dependence of the eikonal. They have been normalized by extrapolating down to the optical point, by using also the slopes mentioned in b). The second group of unnormalized differential cross-section data is that of Ref. 11. Its importance consists not only in giving the form of $d\sigma/dt$ at intermediate t values, but also in supplying the position of the first interference minimum. When compared with the other ones, there data show some systematic tendency to bending downword at the smallest t values. In normalyzing them, we have taken this effect into account and, excepting these lowest-t points, we could see that they agree well with the other existing data.

These data have been divided, according to their energy, into six distinct groups represented by the average center-of-mass energies $\sqrt{s}$ = 19.5, 23, 30.8, 44.8, 53 and 62 GeV. Each group of data is then parametrized as described in the next section and, after this, analyzed all together.

## III. ANALYSIS AND RESULTS

In order to supply gaps in the available experimental informations, following assumptions have been made in the present analysis.

1) As the energy increases, the amplitude varies smoothly.

2) The amplitude is purely imaginary with two simple zeros.

The first assumption means the absence of any remarkable interaction mechanism, which abruptly changes the collision at definite energies. Since we do not know any such mechanism in the range considered here and, whenever data exist to test this requirement, they do fulfil it, this assumption seems us natural.

The second assumption is actually composed of two parts: a) pure imaginary amplitude and b) with two zeros. A direct information about the real part of the amplitude is only available in the forward direction[8,16] where its contribution to the differential cross section is always less than 1% in the entire energy range we are considering. For non-foward direction, existing calculations[17,18] based on dispersion relations and derivative analyticity relations seem to indicate that, as far as $d\sigma/dt$ is concerned, the real part of the amplitude may be significant only in the neighbourhood of the minima of $d\sigma/dt$. Thus, we believe that the omission of the real part does not seriously affect the results. About the number of zeros, it has been pointed out by Durand and Lipes[19] that, in order that the Fourier transform of the

opacity remained always positive, the amplitude should change its sign an even number of times. In that paper, this was fundamental since their proposal was $\chi \sim \langle F^2 \rangle$ as in Ref. 1. Although we did not have such a restriction, we have nevertheless adopted the same criterium in determining $\chi$. It is clear that, if eq. (1) is valid, with $\chi_o(b) \sim \langle F^2 \rangle$, we must necessarily have such an amplitude. Having accepted the above assumption, there still remains the question of the exact number of zeros. The amplitude may have no zeros[18] remaining always positive. In this paper, we have taken a more orthodox view, changing its sign at the first minimum of $d\sigma/dt$. In this case, we must have at least one more zero somewhere. There is an indication of the second minimum[10] of $d\sigma/dt$ around $-t = 8$ GeV$^2$ at $\sqrt{s} = 53$ GeV, but in a similar measurements[15] at $\sqrt{s} = 19.5$ GeV, there is no such indication up to $-t = 12$ GeV$^2$. In the present analysis, we have assumed the second zero of the amplitude were indeed at $-t = 8$ GeV$^2$ for $\sqrt{s} = 53$ GeV, whereas for $\sqrt{s} = 19.5$ GeV, it were at $-t = 12$ GeV$^2$. For the other values of energy, we have made a logarithmic interpolation as shown in Fig. 2. In the same figure, the energy dependence of the position of the first minimum is also displayed, showing that it is consistent with a logarithmic decrease. Actually, the exact position of the second zero of the amplitude, as well as the possible existence of other zeros, have little practical importance, because the experimental uncertainties at smaller values of t are too large to allow such refinements.

Besides the two assumptions mentioned above, we have also neglected the spin dependence, which may affect large - t data, but presumably negligible in the final results on the opacity.

The amplitude has then been written as a sum of gaussians, that is,

$$a(s,t) = a(s,0) \sum_{i=1}^{6} \alpha_i \exp(\beta_i t) \qquad (2)$$

where a(s,t) is related to $d\sigma/dt$ by

$$\frac{d\sigma}{dt} = \pi |a(s,t)|^2 \qquad (3)$$

and the parameters a(s,o), $\alpha_i$ and $\beta_i$ have been determined at each energy value, by fitting the data listed in the preceding section. We summarize the results in Table I. Comparison of our parametrization with data at two energies are made in Figs. 3,4,5 and 6.

Once the amplitude has been determined, we could compute the opacity following the conventional procedure, getting

$$\chi(s,b) = -\log[1 + i\langle a(s,t)\rangle]$$

$$= -\log\left[1 + i\int \frac{d^2k}{2\pi} a(s,t=-\vec{k}^2)\exp(i\vec{b}\cdot\vec{k})\right] \qquad (4)$$

or, by using eq. (2):

$$\chi(s,b) = -\log\left[1 - |a(s,0)| \sum_{i=1}^{6} \frac{\alpha_i}{2\beta_i} \exp\left(\frac{-b^2}{4\beta_i}\right)\right] \qquad (5)$$

Results of this calculation at several values of

b, by using the parameters listed in Table I, are shown in Fig. 7. As can be seen there, a logarithmical increase of $\chi(s,b)$ is consistent with them in the entire range of b, suggesting a parametrization of the form

$$\chi(s,b) = \chi_f(b) + \log\left(\frac{s}{s_0}\right)\chi_0(b) \qquad (6)$$

where $\chi_f(b)$ and $\chi_0(b)$ are functions of the impact parameter alone, not necessarily identical each other. $s_0$ in eq. (6) is some scale factor, which can be taken, for instance, the threshold value $s_0 = (2m_p+m_\pi)^2 \approx (2m_p)^2$. In a previous work[3], where we have studied a classical source model, this constant appeared naturally and with the same order of magnitude. We have indeed adopted this parametrization and, by using the least-square method, fitted it to the points which have been obtained before, according to eq. (5). The resulting curves for $\chi_f(b)$ and $\chi_0(b)$ are displayed in Fig. 8. The main features of there results are: i) $\chi_0(b)$ is much smaller than $\chi_f(b)$; ii) $\chi_0(b)$ is much more peripheral as compared with $\chi_f(b)$.

Going back to Fig. 7, one may feel that the lowest energy points, those corresponding to the NAL data, are systematically in conflict when compared to the other points. A small (~0.5 mb) deviation which appears in the total cross-section data (Fig. 1) may be another indication of this discrepancy. Since these data have been obtained with a different machine, such a discrepancy is perfectly conceivable and, in order to avoid a possible distortion of results, we have also performed a calculation by omitting the NAL data.

As seen in Fig. 8, the neglect of these data did not change the results stated above in any significant way. The only modification is that the central depression of $\chi_o$ has now disappeared.

## IV. COMPARISON WITH SOME OTHER RESULTS AND MODELS

We now proceed comparing the results obtained in preceding section with some earlier results.

First of all, factorized eikonal such as the one given by eq. (1) and used by some authors[2] is discarded by our results. Yet, we observe here that if one would be contented only in a crude analysis of data, the factorization hypothesis may be useful. The existence of some results which favour factorized eikonal[20] as well as some other ones with non-factorized eikonal, but with the second conclusion at the end of section III inverted[21], is an indication of the above statement. We shall come back to the discussion of these works soon after. Anyhow, let us emphasize that if all the existing experimental informations are properly taken into account, they do tell us more than such a rough result.

In recent works[21], Chou has analysed mainly data from Ref. 9 and concluded that the energy dependent part of the eikonal is more central than its constant part. In our opinion, however, the small-t cross section should be more carefully treated. In one of his analyses, the slope parameter B in the very small-t intervals decreases with the incident energy, in an evident opposition to the existing data shown in Fig. 1. For instance, according to his parametrization, the slope parameter in the interval $0.05 < -t < 0.1$ becomes B = 12.50, 11.92 and 11.88 $GeV^{-2}$ for $\sqrt{s}$ = 23, 53 and 62 GeV, respectively. This decrease of B, when combined with the increase of $\sigma_T$, clearly gives an eikonal which increases centrally. In the more recent version, he does consider a shrinking angular

distribution, but it seems us that the slope parameter for $\sqrt{s}$ = 62 GeV has not been taken sufficiently large. It is not clear what has exactly been done there, but if the value $B = 12.40 \pm 0.30$ GeV$^{-2}$ for $\sqrt{s}$ = 53 GeV and interval $0.06 < -t < 0.11$, given by Ref. 5, has been extrapolated down to t=0 and used for $\sqrt{s}$ = 62 GeV, we think this value is definitely too low as is clear in Fig. 1.

In some earlier works[18,22] a peripheral increase of cross section has been pointed out. In all of them, however, the discussion goes around the overlap function and does not refer to the eikonal. It is clear that, even when the energy variation of the eikonal is central, the one corresponding to the overlap function may appear peripheral, Thus, the ambiguity should be removed by discussing directly the opacity, if one intended to consider the internal structure of the interacting hadross.

Another hypothesis which has often been used in analysing the impact structure of hadron-hadron collisions is the geometrical scaling[23]. While this hypothesis becomes more reasonable (at least as an approximation) when stated in terms of the overlap function, since there is a limiting value at the origin which is almost reached at the ISR energies, its validity also in terms of the eikonal has been claimed in Ref. 24, which is not obvious and must be carefully investigated. Our conclusion is that, if one neglects the 1% increase in $\chi(b=0)$ in the interval $\sqrt{s}$ = 20 ~ 62 GeV, the geometrical scaling of the eikonal is quite reasonable. However, if one considers only the ISR data, omitting those at $\sqrt{s}$ = 19.5 GeV, some systematic deviations are observed. Namely, in order to obtain the opacity at $\sqrt{s}$ = 62 GeV, the one calculated at

$\sqrt{s}$ = 23 GeV must be stretched, not uniformly as stated by the geometrical scaling, but in a way that the large impact-parameter points are less expanded than the small impact-parameter ones. Compared to the ratio $\sqrt{\sigma_T(62)/\sigma_T(23)}$, the expansion factor is about 7% larger at $b \simeq 0.5$ f and 2% smaller at $b \simeq 2$ f. It should also be noted that, if we seriously consider the second minimum, which appears in the $\sqrt{s}$ = 53 GeV data[10] around $-t = 8 \sim 9$ GeV$^2$, then the position of this minimum decreases too fast as compared with the geometrical scaling hypothesis ($t_2 \sim \sigma_T^{-1}$), since no such minimum has been observed at $\sqrt{s}$ = 19.5 GeV up to $-t$ = 12 GeV$^2$.

In short, we think our results are more systematic and impartial when compared with the existing analyses, in the sense that we have considered here basically all the published data, including those which have been obtained more recently, avoiding as much as possible biases which may characterize certain groups of data. While the factorization hypothesis for the eikonal is definitely discarded, provided the assumptions introduced in section III are valid, the soundness of the geometrical scaling hypothesis remains not conclusive, although there are indications of its breakdown.

## V. TWO-COMPONENT MODEL

In a previous paper[3], we have discussed a model for high-energy hadron-hadron collisions, where two independent interaction mechanisms were considered: a) pionization, depicted as an excitation of the meson field induced by a classical source representing the incident particles in interaction and b) fragmentation, described as a two-stage process consisting of an incident-particle excitation followed by its decay. We have shown that the first mechanism gives accounts for the increase of the cross sections with the energy, whereas the second mechanism has been assumed to give a constant background to these.

Explicitly, we have written the S matrix (in the impact-parameter representation) as

$$S = S_1 S_2 S_\pi \tag{7}$$

with $S_1$, $S_2$ and $S_\pi$ commuting among them. Here, $S_i$ refers to the fragmentation of the i-th incident particle and $S_\pi$ to the pionization.

The pionization has been computed by solving a classical (scalar) source equation

$$(\Box + \mu^2)\varphi(x) = J(x,\vec{b}) \tag{8}$$

with

$$J(x,\vec{b}) = g|\vec{\pi}_1 - \vec{\pi}_2| \rho_1(x) \rho_2(x) \tag{9}$$

where

$$\rho_i(x) = \gamma_i \, \rho\left[\gamma_i(\vec{x}_\parallel - \vec{v}_i x_0) + (\vec{x}_\perp \pm \frac{\vec{b}}{2})\right] \qquad (10)$$

is a function somehow related to the matter distribution of the i-th particle with velocity $\vec{v}_i$*. For the elastic scattering, the pionization part of the S matrix could be written

$$S_\pi = \exp\left[-\chi_\pi(s,\vec{b})\right] \qquad (11)$$

with

$$\chi_\pi(s,\vec{b}) = \frac{1}{2}\int \frac{d^3k}{2\omega} \left| j(\vec{k},\vec{b}) \right|^2 \qquad (12)$$

where $j(\vec{k},\vec{b})$ is the Fourier transform of $J(x,\vec{b})$.

Now, independently of the detailed form of $\rho_i$, eqs. (9) and (10) imply that $j(\vec{k},\vec{b})$ be asymptotically of the form (in the c.m. system)

$$j(\vec{k},\vec{b}) = j\left(\frac{k_\parallel}{\gamma}, \vec{k}_\perp, \vec{b}\right) \qquad (13)$$

where $\gamma = \sqrt{s}/2m_p$, that is the $k_\parallel$ range in which j is significant expands proportionally to $\sqrt{s}$. Since the energy dependence of $\chi_\pi$ arises from the $k_\parallel$ integration of eq. (12), which is roughly $\sim \int dk_\parallel / k_\parallel$, the upper limit being determined by the cutoff factor $\left| j(\vec{k},\vec{b}) \right|^2$, the final result of

---

* $\gamma_i = (1 - v_i^2)^{-1/2}$

integration gives

$$\chi_\pi(s,\vec{b}) \simeq \log\left(\frac{s}{s_0}\right)\chi_0(b) \tag{14}$$

The fragmentaion has been assumed to give a constant contribution to the elastic channel, namely[3]

$$|\langle p|S_1|p\rangle|^2 = |\langle p|S_2|p\rangle|^2 = \exp[-\chi_f(b)] \tag{15}$$

Thus, the elastic amplitude is altogether written as

$$a(s,t=-\vec{k}^2) = \frac{i}{2\pi}\int d^2b \exp(i\vec{b}\cdot\vec{k})\{1-\exp[-\chi(s,b)]\} \tag{16}$$

where $\chi(s,b)$ is precisely given by eq. (6).

In the previous work, we have adopted a very simple (gaussian) parametrization for $\chi_f$ and $\rho$ (or equivalently for $\chi_0$), namely

$$\chi_f = C\exp(-\beta b^2)$$
$$\chi_0 = A\exp\left(\frac{-b^2}{4\alpha}\right) \tag{17}$$

which gave

$$\log s_0 = \gamma + \log(2\alpha m_p^2 \mu_1^2) \tag{18}$$

where $m_p$= proton mass, $\mu_1^2 = \langle \mu^2 + k_\perp^2 \rangle_{av.}$ and $\gamma$ denotes the Euler's constant. With the parameters in eqs. (17) chosen as C=1, $\beta^{-1}$=13 GeV$^{-2}$, A=4.44x10$^{-2}$ and $\alpha$ =8.5 GeV$^{-2}$, we could reproduce $\sigma_T$, $\sigma_{el}$, $\sigma_{in}$ and $d\sigma/dt$ ($-t \lesssim 0.5$ GeV$^2$) in the

entire s range considered in the present paper.

Although our calculation did depend on this particular parametrization, the results given by eq.(16) plus eq. (6) would remain basically valid (with essentially the same $s_o$) if we have chosen another parametrization. Thus, the conclusions reached in sec. III constitute an additional support of this model and they complement the foregoing results, giving a more precise structure to the opacity.

Let us, then, interpret the results exposed in section III, in terms of our two-component model. First, let us tentatively identify, following Chou and Yang in the original version[1], $\chi_f \sim \langle F^2 \rangle$, that is we are assuming that, before the opacity begins to increase, it is related to the matter distribution inside proton in exactly the way proposed by those authors. Taking for F the dipole formula, we can readily obtain its Fourier transform[19]

$$\langle F^2 \rangle \sim (\lambda b)^3 K_3(\lambda b) \qquad (19)$$

which is shown in Fig. 8.

It can be seen that our $\chi_f$ is slightly narrower than the result predicted with $\lambda^2 = 0.71$ GeV$^2$. Actually, it practically coincides with the curve so calculated with $\lambda^2 \simeq 1$ GeV$^2$, as in Durand and Lipes paper. This means that, as far as the fragmentation is concerned, the matter distribution inside a proton is more compact than the charge dis-

tribution* or, in other words, only when the collision is central, the fragmentation occurs. This is reasonable since such a collective process is really expected to happen only when all the particle interacts.

Next, let us consider the pionization. If one neglects the depression which appears in the central region, $\chi_0(b)$ may well be approximated by a gaussian $\exp(-0.0291\ b^2)$ which corresponds in its turn to $\rho(x)$ in eq. (10) with the same gaussian form above. In terms of average radius, $\bar{r} \simeq 1.15$ f, so this distribution is broader in comparison with the part which is responsible for the fragmentation. That is, the pionization as depicted in our model is a peripheral process.

---

* Here, we are assuming the usual relation between the charge distribution and the form factor[25]. However, a somewhat different relation, which has been proposed recently[26] gives an even more compact distribution, in relation to the one obtained here.

REFERENCES

1) T.T.Chou and C.N.Yang, in Proceedings of the 2nd. International Conference on High Energy Physics and Nuclear Structure, Rehovoth,Israel 1967, G.Alexander, ed. (North-Holland, Amsterdam, Netherlands, 1967) pg. 347; Phys.Rev.170 (1968) 1591.

2) F.Hayot and U.P.Sukhatme; Phys.Rev.D10 (1974) 2183.

3) H.M.França and Y.Hama; preprint IFUSP/P-66 (Dec/1975); Rev. Bras.Fís. 8 (1978) 127.

4) CERN-Pisa-Rome-Stony Brook Collaboration, Phys.Letters 62B (1976) 460.

5) G.Barbiellini et al.; Phys.Letters 39B (1972) 663.

6) U.Amaldi et al.; Phys.Letters 36B (1971) 504.

7) M.Holder et al.; Phys.Letters 36B (1971) 400.

8) U.Amaldi et al.; Phys.Letters 66B (1977) 390.

9) N.Kwak et al.; Phys. Letters 58B (1975) 233.

10) H.De Herret et al.; Phys.Letters 68B (1977) 374.

11) A.Böhm et al.; Phys.Letters 49B (1974) 491.

12) A.S.Carrol et al.; Phys.Letters 61B (1976) 303.

13) V.Bartenev et al.; Phys.Rev. Letters 31 (1973) 1088.

14) C.W.Akerlof et al.; Phys.Rev. D14 (1976) 2864.

15) J.L.Hartmann et al.; Phys.Rev.Letters 39 (1977) 975.

16) V.Bartenev et al.; Phys.Rev.Letters 31 (1975) 1367.

17) J.B.Bronzan, G.L.Kane and U.P.Sukhatme; Phys.Letters 49B (1974), 272.

18) W.Grein, R.Guijas and P.Kroll; Nucl.Phys. B89 (1975) 93.

19) L.Durand and R.Lipes; Phys.Rev. Letters 20 (1968) 637.

20) A.W.Chao and C.N.Yang; Phys.Rev. D8 (1973) 2063.

21) T.T.Chou; Foundations of Physics 8 (1978) 319; T.T.Chou, Nucl.Phys. B139 (1978) 260.

22) U.Amaldi; Proceedings of the 2nd.International Conference on Elementary Particles, Aix-en-Provence (1973); R.Henzi and P.Valin; Phys.Letters B48 (1974) 119; H.I.Miettinen; Proceedings of the 9th. Rencontre de Moriond, Méribeil les Allues (1974).

23) J.Dias de Deus; Nucl.Phys. B59 (1973) 231.

24) J.Dias de Deus and P.Kroll; Phys. Letters B60 (1976) 375.

25) F.J.Ernst, R.G.Sachs and K.C.Wali; Phys.Rev. 119 (1960) 1105.

26) H.M.França, G.C.Marques and A.J.da Silva; "Connection between elastic relativistic form factors and charge distribution", preprint IFUSP/P-137 (1978).

TABLE CAPTION

TABLE I: The parameters defining the amplitude given by eq. (2) and which have been fixed by fitting the published experimental data as explained in the text.

FIGURE CAPTIONS

FIG.1 - The experimental data on the total cross section (above) and the small-t slope parameter (below) which have been used in the present analysis. The t interval where the slope parameter has been measured is not fixed, but depends on the energy and on the experiment.

FIG.2 - In the upper part, we show the existing data on the position of the first minimum of $d\sigma/dt$ as a function of the center-of-mass energy. They are roughly on a straight line. In the lower part, the position of the second minimum, which has been used here, is displayed. At $\sqrt{s}$=53GeV, the cross indicates its value which appears in Ref. 10); at $\sqrt{s}$=19.5 GeV, the cross indicates the highest - t value where $d\sigma/dt$ has been measured[15]. An interpolation to other values of the energy is indicated by the straight line and the arrows.

FIG.3 - The elastic cross section given by eqs.(2) and (3) with the parameters listed in Table I, at $\sqrt{s}$=19.5 GeV. Experimental data are also displayed for comparison.

FIG.4 - The same as Fig.3, but for large t. Near the minima, the real part of the amplitude is expected to dominate.

FIG.5 - The elastic cross section given by eqs. (2) and (3) with the parameter listed in Table I, at $\sqrt{s}$=53GeV. Esperimental data are also shown for comparison.

FIG.6 - The same as Fig. 5, but for large t. Near the minima, the real part of the amplitude is expected to dominate.

FIG.7 - The energy dependence of the eikonal $\chi(s,b)$, which has been calculated with the use of eq. (5), for several values of the squared impact parameter. The straight lines are fits in terms of eq. (6).

FIG.8 - $\chi_f(b)$ and $\chi_0(b)$ which appear in eq. (6), as determined in the present analysis. For $\chi_0(b)$, we show two version, one including all the data mentioned in section II (solid line) and the other excluding the NAL data (dotted line). For comparison we also display the opacity predicted by the dipole formula with $\lambda^2=0.71$ GeV$^2$ (broken line). The error bars which appear in $\chi_f$ and $\chi_0$ include just the fluctuations which appear in Fig. 7.

TABLE I

| $\sqrt{s}$ (GeV) | 19.5 | 23 | 30.7 | 44.9 | 53 | 62 |
|---|---|---|---|---|---|---|
| $\|a(S,0)\|$ ($GeV^{-2}$) | 7.97 | 8.03 | 8.25 | 8.52 | 8.69 | 8.80 |
| $\alpha_1$ | 0.16412 | 0.16412 | 0.16412 | 0.16411 | 0.16411 | 0.16411 |
| $\alpha_2$ | 0.77601 | 0.77601 | 0.77600 | 0.77597 | 0.77597 | 0.77594 |
| $\alpha_3$ | 0.06893 | 0.06893 | 0.06893 | 0.06893 | 0.06893 | 0.06893 |
| $\alpha_4$ | -0.00838 | -0.00838 | -0.00838 | -0.00838 | -0.00838 | -0.00838 |
| $\alpha_5$ | -0.00076 | -0.00076 | -0.00076 | -0.00076 | -0.00076 | -0.00076 |
| $\alpha_6$ | 0.00008 | 0.00008 | 0.00009 | 0.00013 | 0.00014 | 0.00016 |
| $\beta_1$ | 12.5 | 12.7 | 12.7 | 13.3 | 14.0 | 14.0 |
| $\beta_2$ | 5.10 | 5.30 | 5.30 | 5.40 | 5.55 | 5.57 |
| $\beta_3$ | 2.60 | 2.65 | 2.65 | 2.85 | 2.90 | 3.00 |
| $\beta_4$ | 1.150 | 1.170 | 1.170 | 1.175 | 1.200 | 1.200 |
| $\beta_5$ | 0.45 | 0.46 | 0.47 | 0.47 | 0.48 | 0.48 |
| $\beta_6$ | 0.26 | 0.26 | 0.26 | 0.26 | 0.26 | 0.26 |

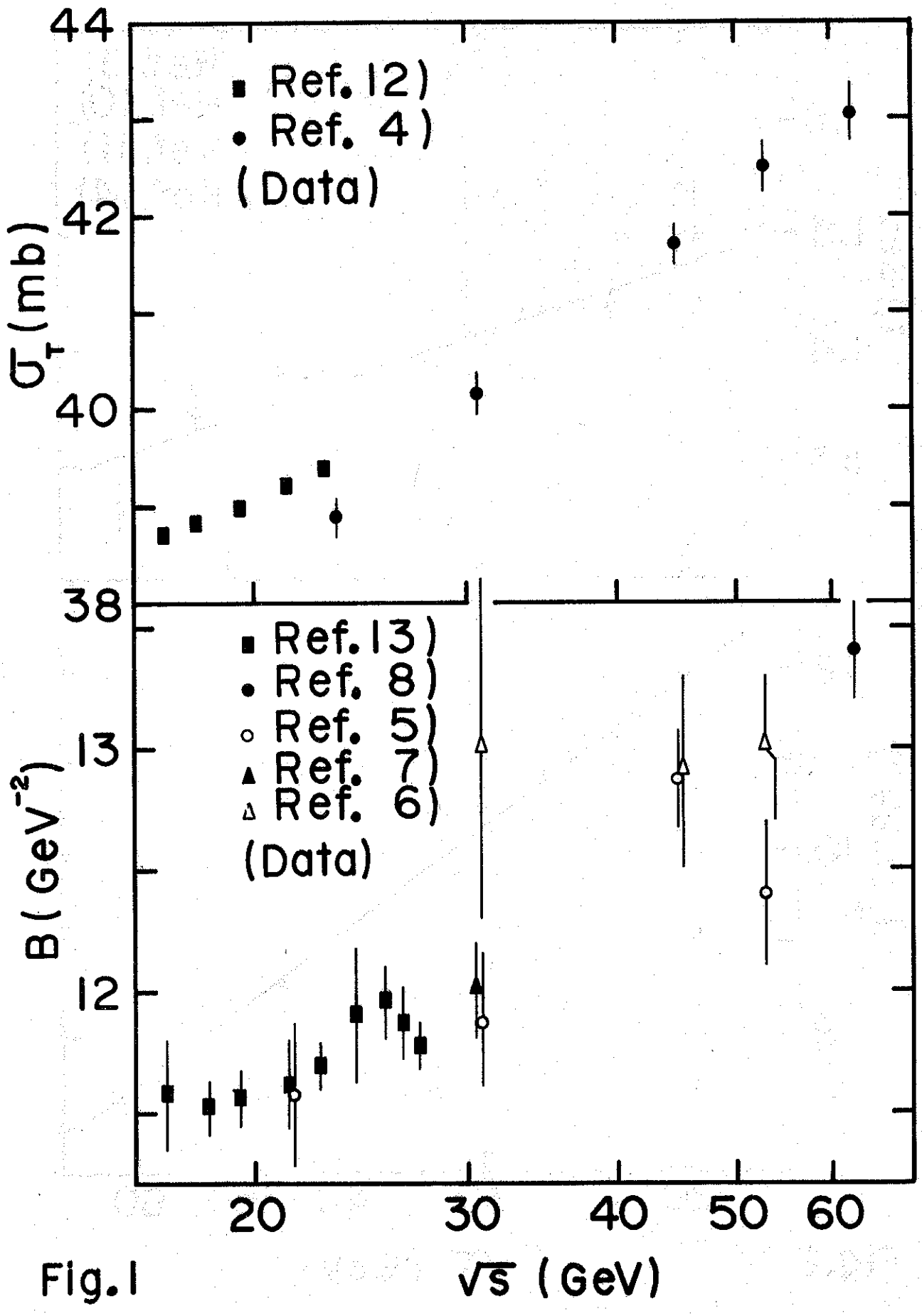
44
42
40
38
13
12
$\sigma_T$ (mb)
B (GeV$^{-2}$)
Ref. 12)
Ref. 4)
(Data)
Ref. 13)
Ref. 8)
Ref. 5)
Ref. 7)
Ref. 6)
(Data)
20
30
40
50
60
$\sqrt{s}$ (GeV)

Fig. 1

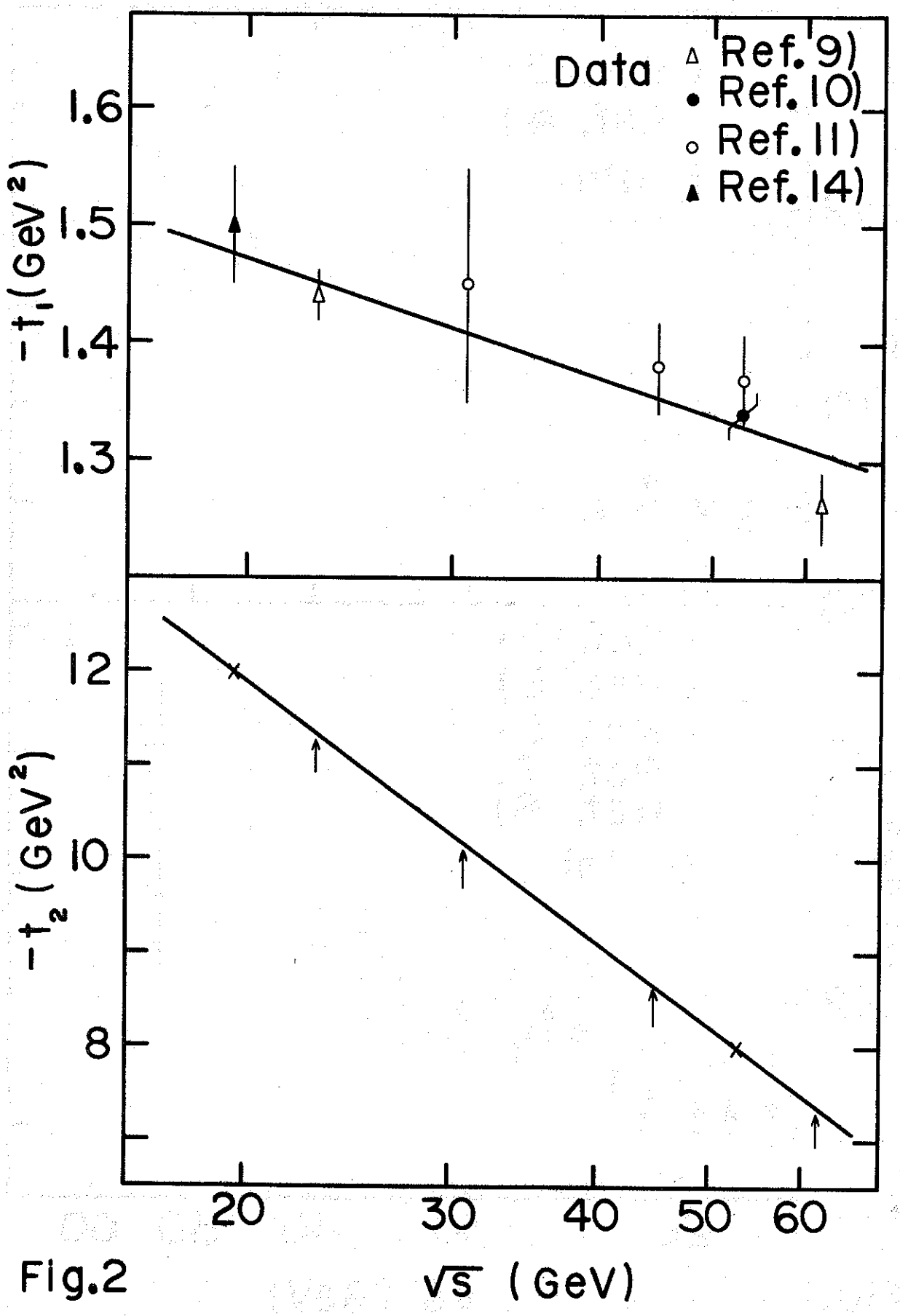
Data
Ref. 9)
Ref. 10)
Ref. 11)
Ref. 14)
$-t_1$ (GeV$^2$)
1.6
1.5
1.4
1.3
$-t_2$ (GeV$^2$)
12
10
8
20
30
40
50
60
$\sqrt{s}$ (GeV)

Fig.2

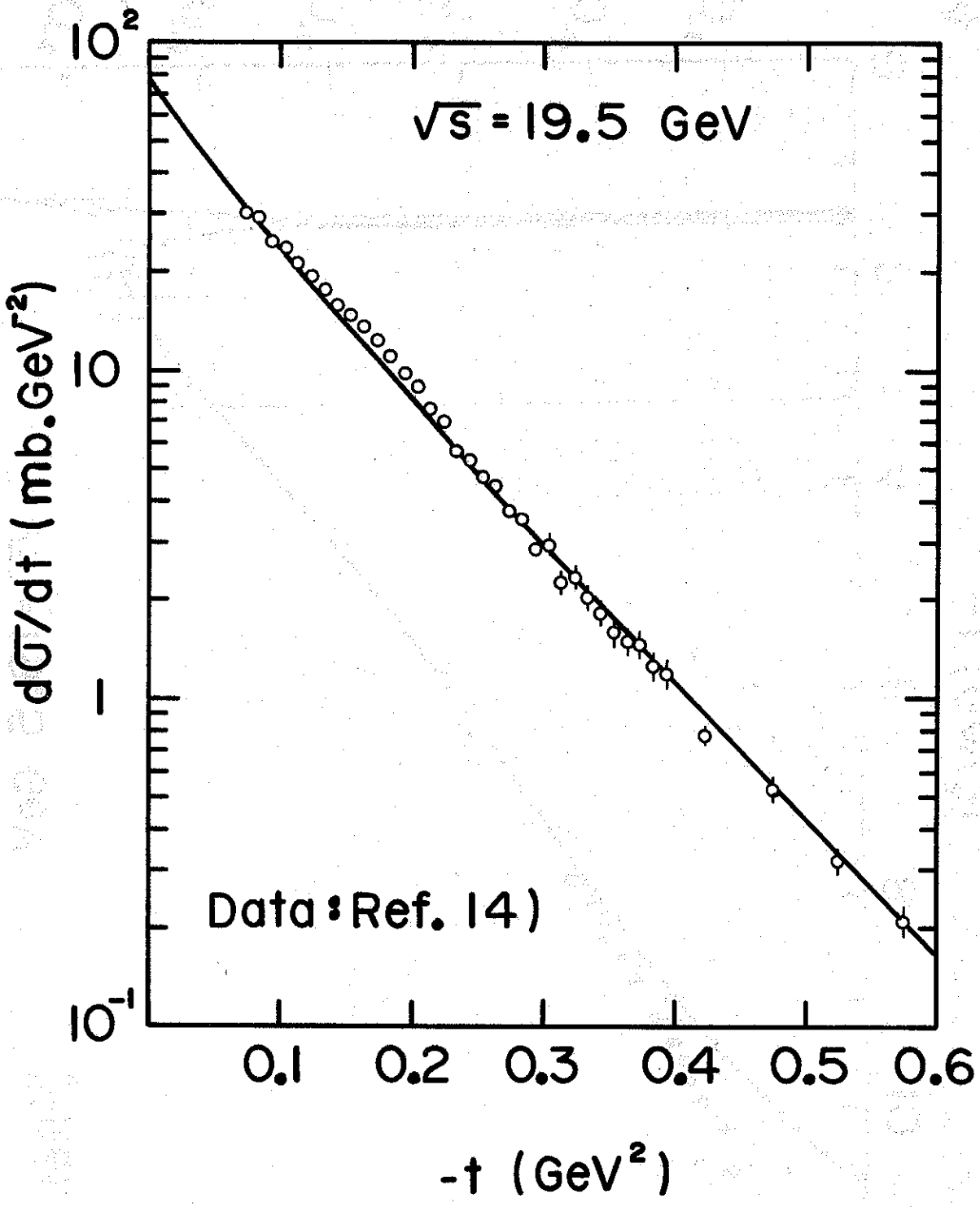
$10^2$
10
1
$10^{-1}$
$\sqrt{s}$ = 19.5 GeV
dσ/dt (mb.GeV$^{-2}$)
Data : Ref. 14)
0.1
0.2
0.3
0.4
0.5
0.6
-t (GeV$^2$)

Fig.3

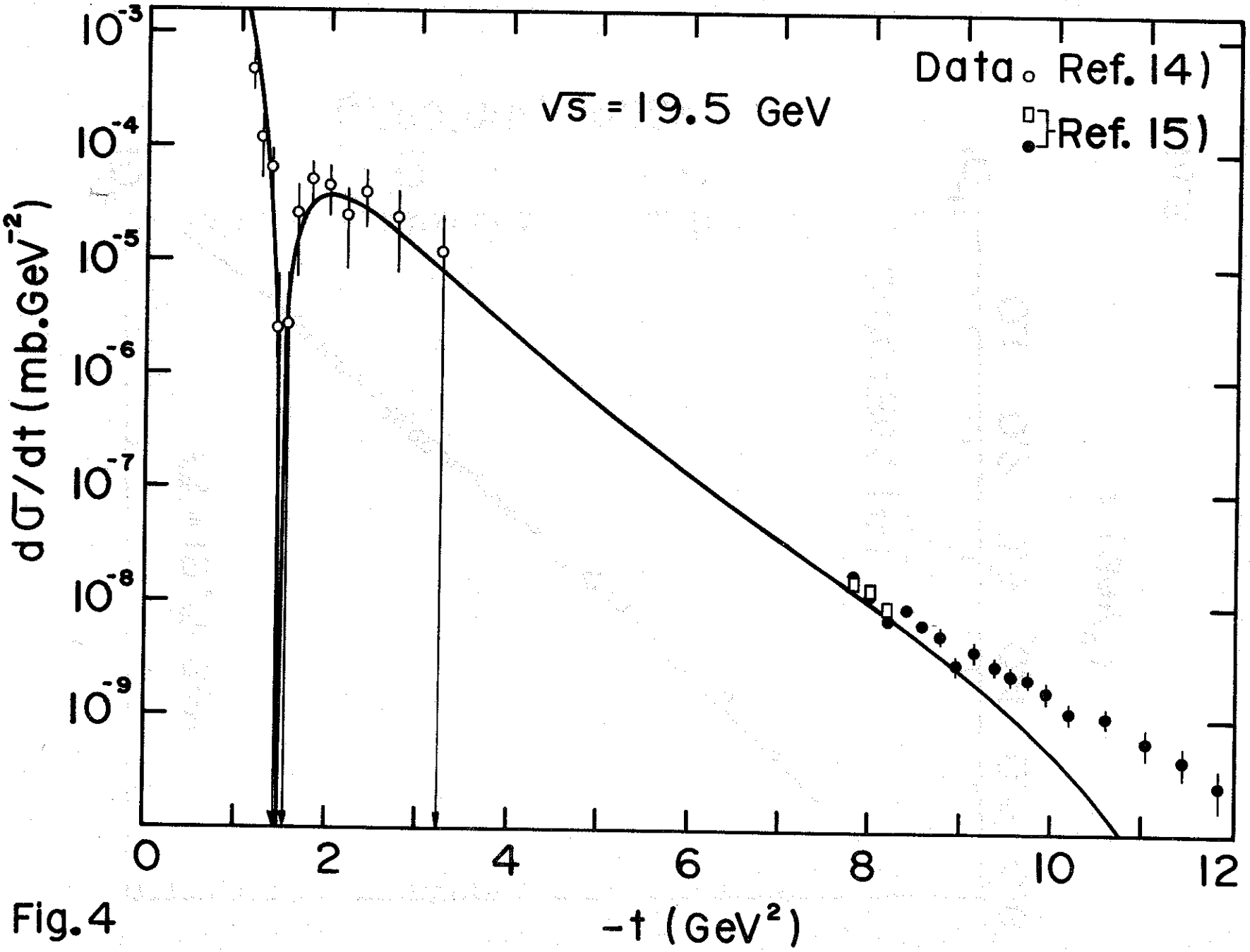
Data. Ref. 14)
Ref. 15)
$\sqrt{s}$ = 19.5 GeV
$d\sigma/dt$ (mb.GeV$^{-2}$)
$10^{-3}$
$10^{-4}$
$10^{-5}$
$10^{-6}$
$10^{-7}$
$10^{-8}$
$10^{-9}$
0
2
4
6
8
10
12
$-t$ (GeV$^2$)

Fig. 4

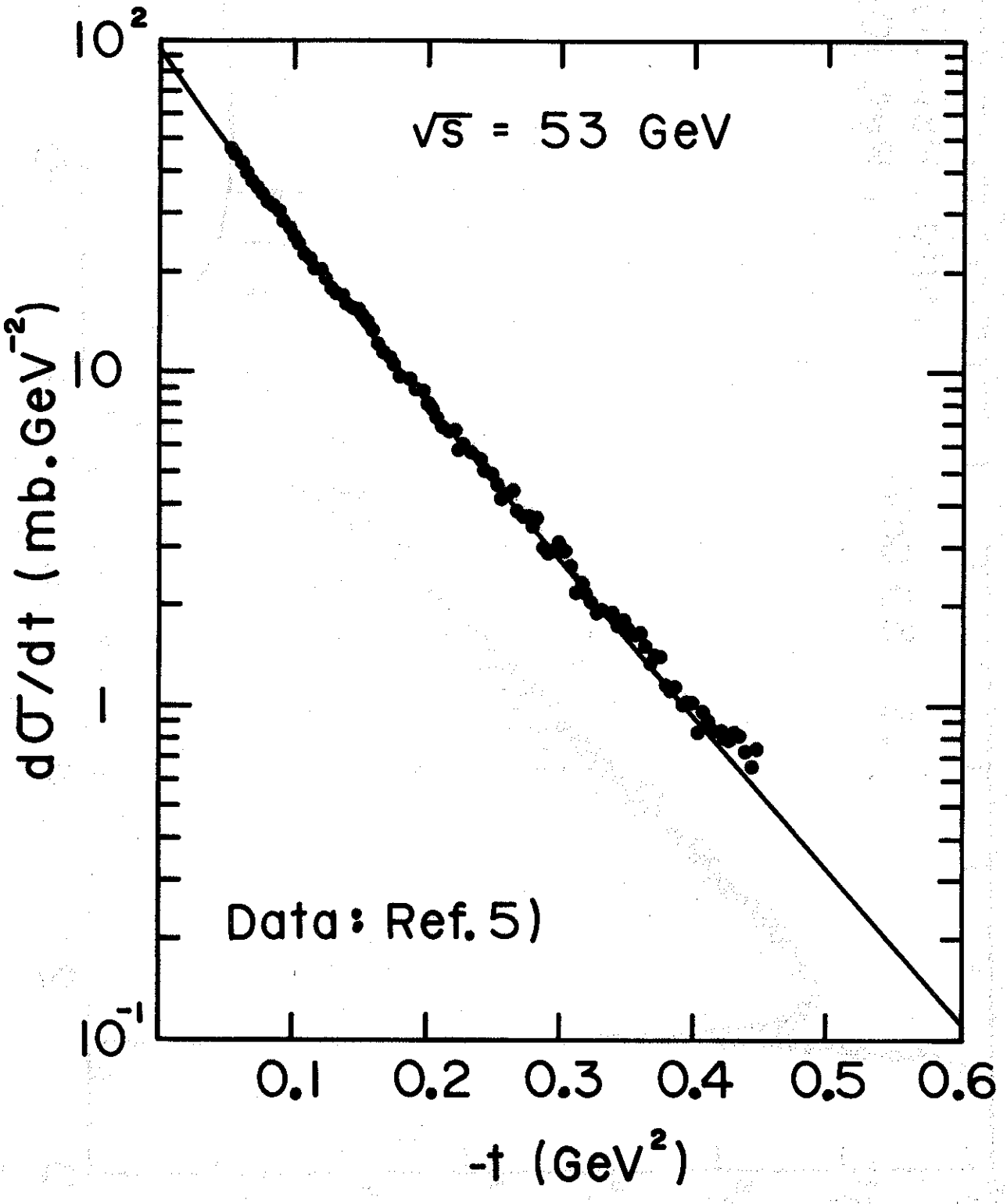
$10^2$
10
1
$10^{-1}$
$d\sigma/dt$ (mb.GeV$^{-2}$)
$\sqrt{s}$ = 53 GeV
Data : Ref. 5)
0.1
0.2
0.3
0.4
0.5
0.6
-t (GeV$^2$)

Fig. 5

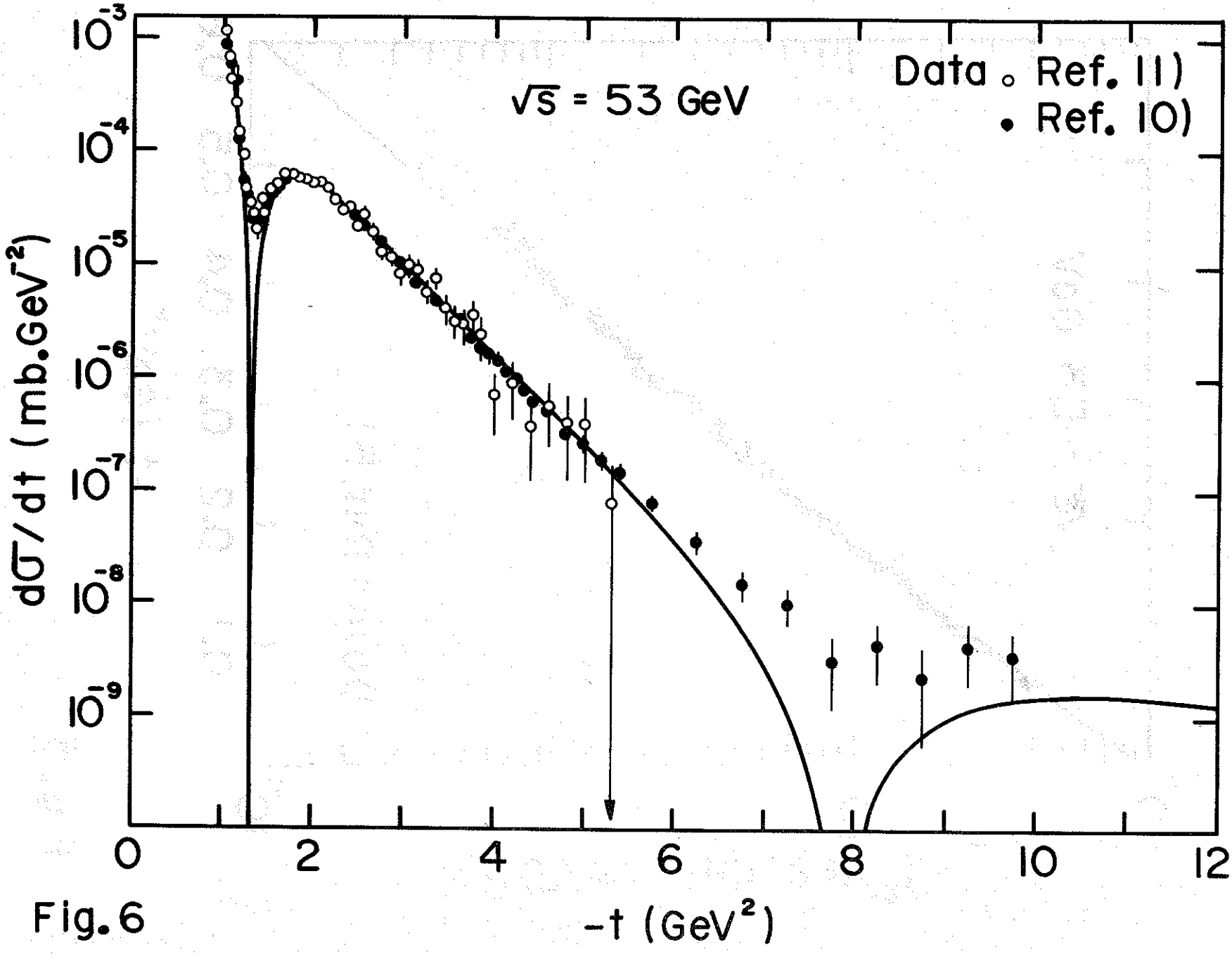
$10^{-3}$
$10^{-4}$
$10^{-5}$
$10^{-6}$
$10^{-7}$
$10^{-8}$
$10^{-9}$
$d\sigma/dt$ (mb.GeV$^{-2}$)
$\sqrt{s}$ = 53 GeV
Data ∘ Ref. 11)
• Ref. 10)
0
2
4
6
8
10
12
$-t$ (GeV$^2$)

Fig. 6

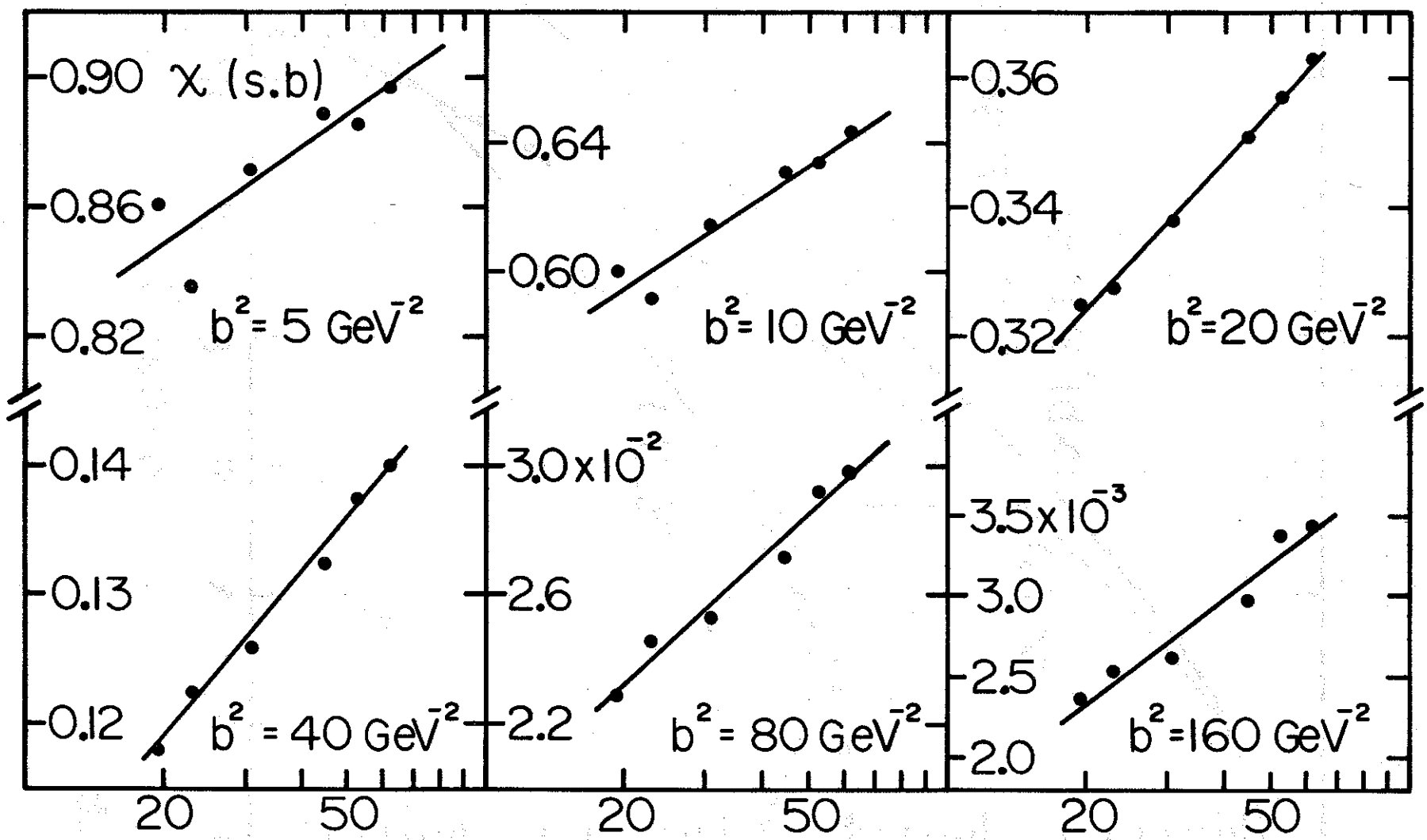
0.90 χ (s.b)
0.86
0.82
$b^2$ = 5 GeV$^{-2}$
0.64
0.60
$b^2$ = 10 GeV$^{-2}$
0.36
0.34
0.32
$b^2$ = 20 GeV$^{-2}$
0.14
0.13
0.12
$b^2$ = 40 GeV$^{-2}$
$3.0 \times 10^{-2}$
2.6
2.2
$b^2$ = 80 GeV$^{-2}$
$3.5 \times 10^{-3}$
3.0
2.5
2.0
$b^2$ = 160 GeV$^{-2}$
20
50
20
50
20
50
$\sqrt{s}$ (GeV)

Fig. 7

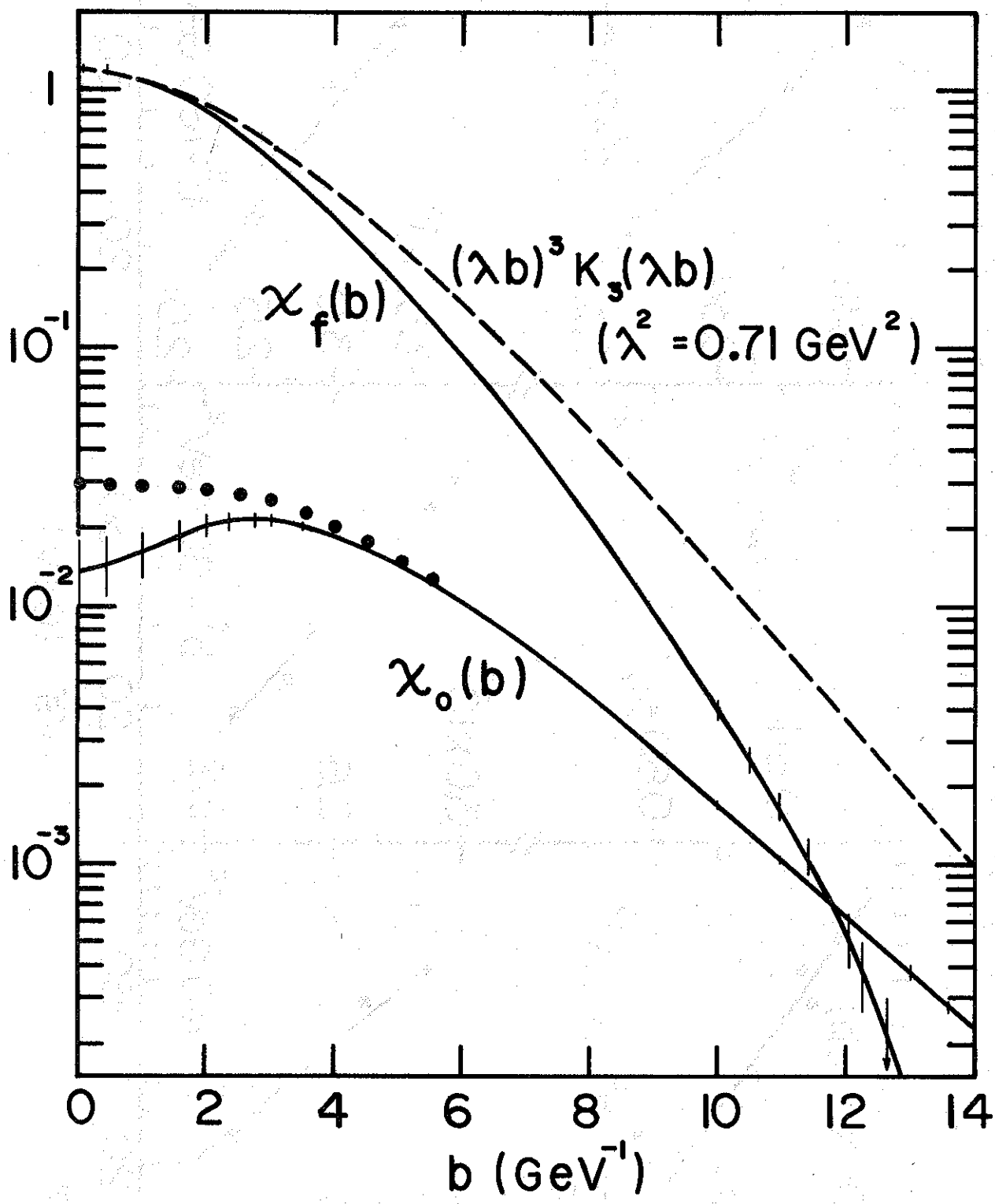
1
$10^{-1}$
$10^{-2}$
$10^{-3}$
$(\lambda b)^3 K_3(\lambda b)$
$(\lambda^2 = 0.71\ GeV^2)$
$\chi_f(b)$
$\chi_o(b)$
0
2
4
6
8
10
12
14
b ($GeV^{-1}$)

Fig.8